

Neuroligin-1 Knockdown Suppresses Seizure Activity by Regulating Neuronal Hyperexcitability

Min Fang · Jin-Lai Wei · Bo Tang · Jing Liu · Ling Chen ·
Zhao-Hua Tang · Jing Luo · Guo-Jun Chen ·
Xue-Feng Wang

Received: 7 September 2014 / Accepted: 12 November 2014 / Published online: 27 November 2014
© Springer Science+Business Media New York 2014

Abstract Abnormally synchronized synaptic transmission in the brain leads to epilepsy. Neuroligin-1 (NL1) is a synaptic cell adhesion molecule localized at excitatory synapses. NL1 modulates synaptic transmission and determines the properties of neuronal networks in the mammalian central nervous system. We showed that the expression of NL1 and its binding partner neurexin-1 β was increased in temporal lobe epileptic foci in patients and lithium-pilocarpine-treated epileptic rats. We investigated electrophysiological and behavioral changes in epileptic rats after lentivirally mediated NL1 knockdown in the hippocampus to determine whether NL1 suppression prevented seizures and, if so, to explore the probable underlying mechanisms. Our behavioral studies revealed that NL1 knockdown in epileptic rats reduced seizure severity and increased seizure latency. Whole-cell patch-clamp recordings of CA1 pyramidal neurons in hippocampal slices from NL1 knockdown epileptic rats revealed a decrease in spontaneous action potential frequency and a decrease in miniature

excitatory postsynaptic current (mEPSC) frequency but not amplitude. The amplitude of N-methyl-D-aspartate receptor (NMDAR)-dependent EPSCs was also selectively decreased. Notably, NL1 knockdown reduced total NMDAR1 expression and the surface/total ratio in the hippocampus of epileptic rats. Taken together, these data indicate that NL1 knockdown in epileptic rats may reduce the frequency and severity of seizures and suppress neuronal hyperexcitability via changes in postsynaptic NMDARs.

Keywords Neuroligin-1 · Temporal lobe epilepsy · NMDAR · Cortex · Hippocampus

Introduction

Epilepsy is the most prevalent chronic neurological disorder, and it is characterized predominantly by recurrent and unpredictable interruptions of normal brain function, called epileptic seizures. Approximately 50 million people worldwide currently have active epilepsy with ongoing seizures that require treatment, and 30 % of epilepsy cases are refractory to drugs [1]. Temporal lobe epilepsy (TLE) is a form of epilepsy that is commonly drug-resistant; TLE is characterized by the occurrence of chronic spontaneous recurrent seizures (SRS) [2]. Epileptic seizures result from an imbalance between excitatory and inhibitory neurotransmission. Increased transmission at glutamatergic synapses, which leads to neuronal hyperexcitability, has been implicated in the pathophysiology of TLE [3], but the detailed regulatory mechanisms responsible for this hyperexcitability are unknown.

Synaptic cell adhesion molecules (CAMs), which are present at synapses and mediate transcellular and intracellular signals, participate in the formation, maturation, function, and plasticity of synaptic connections [4]. Neuroligins (NLs) and neurexins (NRXs) are the best-known CAMs and may

M. Fang
Department of Emergency and Intensive Care Unit, The First Affiliated Hospital of Chongqing Medical University, 1 You Yi Road, Chongqing 400016, China

J.-L. Wei
Department of Gastrointestinal Surgery, The First Affiliated Hospital of Chongqing Medical University, 1 You Yi Road, Chongqing 400016, China

B. Tang · J. Liu · L. Chen · J. Luo · G.-J. Chen · X.-F. Wang (✉)
Department of Neurology, The First Affiliated Hospital of Chongqing Medical University, 1 You Yi Road, Chongqing 400016, China
e-mail: wangxfyp@163.com

Z.-H. Tang
Department of Neurosurgery, The First Affiliated Hospital of Chongqing Medical University, 1 You Yi Road, Chongqing 400016, China

regulate the fine balance between neuronal excitation and inhibition [5, 6]. NLs are receptors for presynaptically localized NRXs; NLs and NRXs interact via their respective ectodomains. Three genes encode presynaptic NRXs, which are differentially expressed in all neurons in α and β forms, and NLs are produced from four genes (NL1–NL4) [7, 8]. NL1 and its binding partner, neurexin-1 β (NRX1 β), are the most widely studied CAMs in the NL and NRX families; NL1 and NRX1 β connect pre- and postsynaptic neurons at excitatory synapses [9]. NL1 is involved in the formation of excitatory synapses, and it may associate indirectly with *N*-methyl-D-aspartate receptors (NMDARs) via a common binding interaction with postsynaptic density-95 (PSD-95) [10, 11]. Previous studies have reported that the number of glutamatergic synapses increases with NL1 overexpression [10, 11] and decreases with NL1 knockdown by RNA interference [12]. NL1 overexpression increases the presynaptic release probability and accelerates the maturation of presynaptic boutons in immature cultured neurons, and presynaptic terminals in NL1 knockout mice exhibit presynaptic immaturity [13]. The cooperation of NL1 and *N*-cadherin is required to increase the release probability and miniature excitatory postsynaptic current (mEPSC) frequency at mature synapses [14]. These studies demonstrate that NL1 participates in the regulation of excitatory transmitter release at glutamatergic synapses.

Some members of the CAM family, including Netrin-G2 and ADAM22, are involved in synaptic transmission and epilepsy [15, 16]. Recent evidence suggests that NRXs and NLs play important roles beyond development, and they are also linked to a variety of human central nervous system (CNS) disorders [17, 18]. Harrison, V. et al. [19] found that compound heterozygous deletion of Nrx1 caused severe developmental delay with early-onset epilepsy. Several studies have found mutations in the NRX or NL genes in patients with familial autism spectrum disorders (ASD) [20, 21]. ASD and epilepsy co-occur in approximately 30 % of individuals with ASD or epilepsy, which suggests that molecular and pathophysiological mechanisms exist that may account for the common co-occurrence of ASD and epilepsy [22]. Thus, we hypothesized that NRXs and NLs are also involved in epilepsy.

We hypothesized that NL1 also participates in the modulation of excitability in CNS neuronal networks via alterations in synaptic transmission during the development of TLE. Thus, we first examined NL1 expression in temporal lobe epileptic foci in TLE patients and experimental animals. Second, we used virus-mediated RNA interference to deplete endogenous NL1 in the hippocampus and investigated electrophysiological and behavioral changes in epileptic rats to further explore the possible role of NL1 in TLE.

Materials and Methods

Human Subjects

Twenty-two patients were selected randomly from a list of 220 patients who had undergone a resection of temporal lobe tissue for intractable TLE after detailed preoperative and intraoperative evaluations and who had donated tissue to our established epilepsy brain bank. The diagnosis of epilepsy was confirmed in these patients according to the 1981 International Classification of Epileptic Seizures by the International League Against Epilepsy. Patients with intractable TLE were eligible for inclusion if they lacked a specific etiology. Patients were excluded if they had progressive lesions in the CNS such as tumors, cortical dysplasia, or vascular malformations in the CNS. The study subjects had all undergone surgical removal of the epileptogenic zone in their temporal lobe as a treatment for their seizures. All patients were refractory to maximal doses of at least three or more antiepileptic drugs (AEDs), including valproate, phenobarbital, carbamazepine, gabapentin, topiramate, phenytoin, lamotrigine, and clonazepam. Presurgical assessments included a detailed history and neurological examination, neuropsychological testing, neuroradiological studies, and interictal and ictal electroencephalogram (EEG) studies. Each patient underwent brain magnetic resonance imaging (MRI; 3.0 T) using routine scan sequences (T1WI, T2WI, and FLAIR) before surgery, and no mass lesions were found in the CNS in any of these patients. Sphenoidal electrode monitoring and intraoperative electrocorticography (ECOG) were performed to localize the epileptic lesion before resection in all patients. Clinical features of the patients are shown in Table 1. Human hippocampal samples were not used in our study for the following reasons. Hippocampal resection is seldom required for surgical treatment of CNS disorders (e.g., Alzheimer's disease, Parkinson's disease, multiple sclerosis, and head trauma), with the exception of intractable epilepsy. Moreover, we did not obtain normal hippocampal specimens as controls because of practical and ethical considerations. Postmortem hippocampal tissues are available, but protein degradation would likely affect the results. Thus, we did not study the hippocampus in TLE patients because of the lack of hippocampal controls.

For comparison, 10 histologically normal temporal neocortex samples were obtained from individuals who had been treated for increased intracranial pressure due to head trauma. None of these subjects had a history of epilepsy, exposure to AEDs, or other neurological diseases. Table 1 shows the clinical features of the control subjects.

All TLE samples were collected from patients in the operating room. The anterior 3.5–4.0 cm of the lateral temporal lobe was resected en bloc from the superior temporal gyrus to the collateral fissure and frozen or fixed quickly after resection. A portion of the excised brain tissue from each TLE

Table 1 Clinical characteristics of TLE patients and control patients

Patients	Age (y)/Gender	SF (/m)	Course (y)	AEDs before surgery	Pathology
1	26/M	5	13	CBZ, TPM, VPA	g, nl
2	19/F	6	6	VPA, LTG, CZP	nl, nd
3	18/M	8	5	VPA, CBZ, TPM, PB	g
4	28/M	3	6	CBZ, TPM, CZP	g, nl, nd
5	32/F	5	19	VPA, PB, CBZ, TPM	g, nl
6	39/M	12	15	VPA, PHT, CBZ	g
7	29/M	8	5	VPA, CBZ, PHT	g, nl
8	17/F	3	8	VPA, CBZ, PB, TPM	g, nl
9	22/M	5	10	VPA, CBZ, LTG	g, nl
10	27/F	7	6	VPA, PB, TPM	g
11	32/M	16	19	VPA, CBZ, PHT	g, nd, nl
12	11/F	25	4	VPA, CBZ, TPM, LTG	g
13	20/M	4	9	VPA, CBZ, TPM, GBP	g, nl, nd
14	42/M	9	10	VPA, PHT, LTG	g, nl
15	34/F	15	9	VPA, PHT, LTG	g
16	16/F	3	6	VPA, PB, TPM	g
17	36/F	12	20	VPA, PB, CBZ, PHT	nl, nd
18	38/M	7	21	VPA, PB, CBZ, LTG	g
19	52/M	9	10	VPA, PHT, LTG	g, nl, nd
20	17/F	16	6	VPA, PB, CBZ, TPM	g, nl
21	23/F	10	14	VPA, CBZ, LTG	g, nl, nd
22	48/M	6	26	VPA, CBZ, TPM, PB	nl, nd
Control	Age (y)/Gender	Etiology diagnosis		Adjacent tissue pathology	
1	19/F	Trauma		n	
2	43/M	Trauma		n	
3	32/F	Trauma		n	
4	27/M	Trauma		n	
5	20/F	Trauma		n	
6	32/M	Trauma		n	
7	47/M	Trauma		n	
8	34/F	Trauma		n	
9	29/F	Trauma		n	
10	21/M	Trauma		n	

F female, M male, SF seizure frequency, y year, m month, VPA valproate, PB Phenobarbital, CBZ carbamazepine, TPM topiramate, PHT phenytoin, LTG lamotrigine, GBP gabapentin, CZP clonazepam, n normal, nl neuron loss, nd neuron degeneration, g gliosis

patient studied was immediately placed in a cryovial and stored in liquid nitrogen until used for western blot analyses. Additional portions of the samples were fixed in 4 % buffered formalin for 48 h, embedded in paraffin, sectioned at 5 µm for immunohistochemical analysis or 10 µm for immunofluorescence analysis, and mounted on polylysine-coated slides. Two sections from each specimen were processed for hematoxylin-eosin staining. All control samples were collected in the operating room from patients who were treated for intracranial hypertension within ~2–4 h after head trauma. The anterior temporal neocortex was resected selectively in these patients and frozen or fixed immediately after resection. Tissue from

these control subjects was processed in a manner similar to that used to process tissue from TLE patients, and there was no difference in the time from tissue collection to processing between the control and TLE groups. One part of the tissue was used for western blot analysis. Another part of the tissue was used for immunohistochemical analysis, immunofluorescence analysis, and hematoxylin-eosin staining. Pathology examinations were also performed to exclude any potential pathological damage in control samples.

This study was approved by the ethics committee for human research at Chongqing Medical University. Informed, written consent was obtained from patients or their relatives

for the use of data and tissue for research, which was performed in accordance with the Declaration of Helsinki of the World Medical Association.

Experimental Animals

Adult male Sprague-Dawley rats (12 weeks old) weighing 180–250 g were obtained from the Experimental Animal Center of Chongqing Medical University, China. The rats were housed in a 12-h light/dark cycle with ad libitum access to food and water. All experiments were performed according to the Commission of Chongqing Medical University for the Ethics of Experiments on Animals in accordance with international standards.

Lithium chloride (127 mg/kg IP, Sigma, USA) was injected 24 h prior to pilocarpine administration (50 mg/kg IP, Sigma). Rats were pretreated with atropine sulfate (1 mg/kg IP, Sigma) 30 min prior to pilocarpine administration, which reduced the peripheral cholinomimetic effects of pilocarpine. Rats received repeated pilocarpine injections (10 mg/kg IP) every 20 min until they developed seizures. Diazepam (10 mg/kg IP) was used to control seizure duration. All experimental animals received injections of 1 mL of 0.9 % NaCl IP immediately following a seizure and twice daily following a seizure to prevent dehydration. Control rats were treated similarly except that they were injected with saline instead of pilocarpine. All animals required special care until they were sacrificed. Evoked behavioral seizures were scored using Racine's scale as follows: 0, no response; 1, ear and facial twitching; 2, myoclonic body jerks; 3, clonic forelimb convulsions; 4, generalized clonic convulsions, turning over onto one side; 5, generalized tonic convulsions. Only seizures that were scored 4 or 5 were considered in this study.

A portion of the rats from each group were sacrificed at different time points following a seizure by decapitation after a lethal dose of chloral hydrate IP. The temporal neocortex and hippocampus were dissected and placed in liquid nitrogen for western blot analyses and real-time quantitative PCR (qRT-PCR) analyses. The remaining rats in each group were anesthetized and intracardially perfused using 0.9 % saline followed by 4.0 % paraformaldehyde. Both sides of the temporal lobe were excised after perfusion and immediately fixed via immersion in 4 % paraformaldehyde. Tissues were embedded in paraffin and sectioned at 5 μ m for immunohistochemical analysis and 10 μ m for immunofluorescence analysis. Two sections from every specimen were processed for hematoxylin-eosin staining.

Immunohistochemistry

Tissue sections were deparaffinized in xylene and rehydrated in a series of graded concentrations of ethanol before staining. Sections were incubated in 0.3 % H₂O₂ for 15 min at 37 °C

and boiled in 10 mmol/L sodium citrate buffer (pH 6.0) for 15 min at 92–98 °C for antigen retrieval. A blocking solution of normal goat serum (Zhongshan Golden Bridge, Inc., Beijing, China) was added to the sections, and the sections were incubated for 30 min at 37 °C. The sections were then incubated with a primary anti-NL1 antibody (mouse monoclonal antibody, 1:100, Santa Cruz, Biotechnology, USA) at 4 °C overnight. Sections were washed in phosphate-buffered saline (PBS) for 5 min and incubated with a biotinylated secondary goat anti-mouse antibody (Zhongshan Golden Bridge, Inc.) for 30 min at 37 °C. The sections were washed in PBS and incubated with an avidin-biotin peroxidase complex (Zhongshan Golden Bridge, Inc.) for 30 min at 37 °C. The sections were washed in PBS and incubated with 3,3'-diaminobenzidine (DAB, Zhongshan Golden Bridge, Inc.) for 3 min. Hematoxylin was used to counterstain nuclei. Primary and secondary antibodies were replaced with PBS as negative controls. A LEICA DM6000B automatic microscope (Leica, Germany) was used to collect images. Cells with buffy stains in the cytoplasm or the cell membrane were considered positive. Ten random visual field images for every sample were analyzed automatically and semiquantitatively using the Motic Med 6.0 CMIAS pathology image analysis system (Beijing Motic, Beijing, China).

Double-Label Immunofluorescence and Confocal Microscopy

The tissue sections were deparaffinized and rehydrated, and antigen recovery was performed as described for the samples processed for immunohistochemistry. Tissues were permeabilized using 0.4 % Triton X-100 for 10 min and then subjected to heat-induced antigen retrieval in 10 mM/L sodium citrate buffer for 20 min at 92–98 °C. Tissue sections were blocked using 5 % bovine serum albumin (Zhongshan Golden Bridge Inc.) for 1 h and then incubated at 4 °C overnight with a mixture of a mouse anti-NL1 monoclonal antibody (1:100, Santa Cruz, Biotechnology) and a rabbit anti-NMDAR1 (NMDAR subunit GluN1) monoclonal antibody (1:100, Epitomics, Burlingame, CA, USA) or a mixture of a mouse anti-NL1 monoclonal antibody (1:100, Santa Cruz, Biotechnology) and a rabbit anti-glial fibrillary acidic protein antibody (GFAP, Zhongshan Golden Bridge, Inc.). Sections were washed using PBS and incubated with DyLight 488-conjugated anti-mouse IgG (1:100, Zhongshan Golden Bridge, Inc.) and DyLight 594-conjugated anti-rabbit IgG (1:100, Zhongshan Golden Bridge, Inc.) in the dark for 4 h at 37 °C. Sections were washed using PBS, mounted, sealed, and dried overnight. Fluorescence-stained sections were examined using confocal laser scanning microscopy (Leica Microsystems Heidelberg GmbH, Germany) on an Olympus IX 70 inverted microscope (Olympus, Japan) equipped with a Fluoview FVX confocal scanhead.

Western Blot Analysis

Whole-cell and membrane protein extraction kits (Keygen Biotech, Nanjing, China) were used with homogenized fresh brain tissues. Protein concentrations were measured using a bicinchoninic acid protein (BCA) assay (Pierce, USA). Electrophoresis was performed using a Mini-Protean system (Bio-Rad Laboratories, Hercules, CA, USA). The protein extracts were separated by sodium dodecyl sulfate-polyacrylamide gel electrophoresis (SDS-PAGE) and electrotransferred onto an Immobilon polyvinylidene difluoride (PVDF) membrane (Millipore Corporation, USA) using an electrophoretic transfer system (Bio-Rad Laboratories). The PVDF membranes were blocked in freshly prepared buffer supplemented with 5 % nonfat dry milk (Boster Bioengineering, Wuhan, China) for 1 h at 37 °C. A mouse anti-NL1 antibody (1:100, Santa Cruz, Biotechnology), a mouse anti-NRX1 β antibody (1:800, NeuroMab, University of California, Davis, Davis, CA), a rabbit anti-NMDAR1 monoclonal antibody (1:100, Epitomics), and a mouse anti- β -actin antibody (1:1,000, Santa Cruz) were used as primary antibodies in this experiment. The PVDF membranes were then incubated with the primary antibodies overnight at 4 °C. The PVDF membranes were washed with a mixture of Tris buffered saline and Tween 20 (TBST) and incubated with a horseradish peroxidase-conjugated secondary antibody in TBST (1:5,000 dilution, goat anti-rabbit IgG-HRP or goat anti-mouse IgG-HRP, Santa Cruz) for 60 min at 37 °C. Protein bands were visualized using an enhanced chemiluminescence substrate kit (Pierce) before digital scanning (Bio-Rad Laboratories). Image pixel density was quantified using Quantity One software (Bio-Rad Laboratories).

qRT-PCR Analysis

NL1 and NRX1 β mRNA expression levels in rat hippocampal tissues were analyzed by qRT-PCR. Rat β -actin expression was measured as a control. The following primer sequences were used: for NL1, forward 5'-TGCCATCAAC AGACATCACTC-3', reverse 5'-TCTACCGAGAAGGGAC TTGG-3'; for NRX1 β , forward 5'-CCTGGGTGACTACCTT GAGC-3', reverse 5'-TCCTCGTGAAACGCCTACA-3'; and for β -actin, forward 5'-ACGGTCAGGTCTACACTATC G-3', reverse 5'-GGCATAGAGGTCTTACGGATG-3'. Total RNA was extracted using Trizol reagent (Takara Bio, DaLian, China) according to the manufacturer's protocol. Total RNA was purified, and cDNA synthesis was performed using a PrimeScript™ RT reagent kit and gDNA Eraser (Takara Bio). Equivalent amounts of cDNA were used for real-time PCR in a 20- μ L reaction volume containing 10 μ L of 2 \times SYBR Premix Ex Taq™ II (Takara Bio) and 1 μ L of specific primer pairs. Real-time quantitative PCR reactions were performed in a 96-well plate using a 35-cycle 2-step

PCR protocol in an iQ Multiplex Powermix system (Bio-Rad Laboratories). Amplification steps were performed using CFX Manager software version 1.6 (Bio-Rad Laboratories). A melting curve was generated, and amplification curves were analyzed at the end of the amplification process. The threshold cycle (C_t) was used to determine the relative expression of each gene, and relative quantities (RQ) were calculated using the $2^{-\Delta\Delta C_t}$ method; $RQ=2^{-\Delta\Delta C_t}$, where $\Delta\Delta C_t=\Delta C_t$ (treated rat sample)- ΔC_t (control rat sample) and $\Delta C_t=C_t$ (NL1 or NRX1 β)- C_t (β -actin).

Lentiviral Vector Injections

Lentiviral constructs used in these experiments were manufactured by Sunbio Medical Biotechnology Co., Ltd. (Shanghai City, People's Republic of China). The target site for RNA interference-mediated suppression of rat NL1 was selected based on previous studies [12, 23] in which small hairpin RNA NL1 (sh-NL1) lentiviral constructs were described. A dual-promoter lentiviral vector containing the small hairpin RNA (shRNA) targeted to NL1, under the control of a U6 promoter, and enhanced green fluorescent protein (EGFP), under the control of a CMV promoter, was used in experiments. A lentiviral vector that expressed EGFP alone was used as a control.

Rats were anesthetized using chloral hydrate and placed in a stereotaxic instrument (Stoelting, Wood Dale, IL, USA). Stereotaxic coordinates were calculated with respect to bregma for the anterior-posterior (A-P) axis, the midline for the medial-lateral (M-L) axis, and the dura for the dorsal-ventral (D-V) axis, with the tooth bar set at D-V -3.3 mm. Viral particles were injected through a glass pipette using a Stoelting microsyringe pump (Stoelting) bilaterally into the dorsal hippocampus (A-P=-3.3 mm, M-L=±1.8 mm, D-V=-2.6 mm) and ventral hippocampus (A-P=-4.8 mm, M-L=±5.2 mm, D-V=-6.4 and -3.8 mm) [24]. The pipette was left in place for an additional 2 min after injection to prevent the backflow of viral particles through the injection track. Normal and vehicle control rats were treated similarly, except that these rats were injected with saline and vehicle virus, respectively.

Western blot analysis of NL1 expression in the hippocampus was used to verify the efficacy and selectivity of the RNA interference for NL1 *in vivo*. A goat anti-EGFP antibody (1:200, Abcam, USA) and DyLight 488-conjugated anti-goat IgG (1:100, EarthOx, USA) were used to identify virus-infected neurons in the hippocampus by immunofluorescence.

Behavioral Assays

After 7 days of recovery following injections, the following three groups were given lithium chloride-pilocarpine injections: the sham operation group that received a hippocampal

injection of saline (EP), the control group that received a hippocampal injection of vehicle virus (EP+sh-con), and the experimental group that received a hippocampal injection of NL1 shRNA (EP+sh-NL1). We scored seizures and measured seizure latency in these three groups for 60 min after pilocarpine injection. Investigators who were blinded to the intervention methods observed rat behavior and seizure-related activities throughout the experimental procedure.

Electrophysiological Studies in Hippocampal Slices

Hippocampal slices were prepared from Sprague-Dawley rats. Briefly, brains were rapidly removed under deep anesthesia, and coronal brain slices (400 μ m thickness) that contained hippocampi were cut using a vibrating blade microtome (Leica VT 1200S) in an ice-cold cutting solution that contained 2.5 mM KCl, 2 mM CaCl₂, 2 mM MgCl₂, 1.25 mM KH₂PO₄, 25.2 mM sucrose, 26 mM NaHCO₃, and 10 mM glucose and was continuously bubbled with carbogen (95 % O₂/5 % CO₂) to adjust the pH to 7.35. Freshly cut slices were transferred to an incubation chamber that contained modified artificial cerebrospinal fluid (ACSF; 125 mM NaCl, 2.5 mM KCl, 1 mM MgCl₂, 2 mM CaCl₂, 1.25 mM KH₂PO₄, 26 mM NaHCO₃, and 25 mM glucose, saturated with 95 % O₂/5 % CO₂, pH 7.35). Slices in ACSF were incubated at 34 °C for 1 h and maintained at room temperature prior to recording.

Whole-cell recordings of CA1 pyramidal neurons in brain slices were performed based on their morphology and location using a MultiClamp 700B amplifier. Whole-cell current-clamp recordings were performed using an internal pipette solution (122.5 mM K-gluconate, 17.5 mM KCl, 2 mM MgCl₂, 0.5 mM EGTA, 10 mM HEPES, 4 mM ATP, with pH adjusted to 7.2 by KOH) for action potential (AP) recordings. Whole-cell voltage-clamp recordings were performed using an excitatory internal pipette solution (132.5 mM Cs-gluconate, 17.5 mM CsCl, 2 mM MgCl₂, 0.5 mM EGTA, 10 mM HEPES, 4 mM ATP, and 5 mM QX-314, with pH adjusted to 7.2 by CsOH) in ACSF containing 10 μ M bicuculline to record excitatory events. mEPSC recordings were performed in the presence of 1 μ M tetrodotoxin (TTX).

We performed whole-cell patch-clamp recordings of CA1 pyramidal neurons in acute hippocampal slices and measured AMPAR- and NMDAR-dependent synaptic responses that were evoked by Schaffer collateral stimulation. The ratio of NMDA receptor-mediated synaptic currents to AMPA receptor-mediated synaptic currents (NMDA/AMPA receptor ratios) is widely used to assess synaptic transmission in different brain slices because this ratio is independent of variables in experimental conditions, such as electrode positioning or brain tissue anatomy. NMDA/AMPA receptor ratios were analyzed in two steps for each neuron. First, we obtained stable synaptic responses at -70 mV; the amplitude of these

responses was the AMPAR-specific component. Second, the holding potential was changed to +40 mV, and we collected dual-component EPSCs. At this step 50 ms poststimulus, when the AMPAR contribution was negligible, the amplitude of the dual-component EPSC was interpreted as the NMDAR-specific component. Alterations of the NMDA/AMPAR ratio could result from changes in either NMDA synaptic currents or AMPA synaptic currents or both. Therefore, we also compared NMDAR-specific components and AMPAR-specific components when the stimulus intensity was set to evoke a similar range of AMPA responses; the NMDAR-specific components were recorded without changing the stimulus intensity.

Data Analysis

Data are expressed as means \pm standard deviation (S.D.). Student's *t* test (SPSS 11.5) was used for statistical analyses of differences between two groups. Differences between groups were also determined using one-way analysis of variance (ANOVA) followed by Tukey's honest significant difference (HSD) post hoc multiple comparison test (SPSS 11.5). Repeated measures ANOVA was used to compare group means of a dependent variable across repeated measurements of time (SPSS 11.5). Fisher's exact test was used to compare two groups of two categorical variables (SPSS 11.5). A value of *p* < 0.05 was considered statistically significant.

Results

Clinical Characteristics and Postoperative Outcomes in Epileptic Subjects

The epilepsy patients studied had a mean age of 28.46 \pm 10.92 years and included 12 male and 10 female patients. The mean time since the onset of seizures was 11.23 \pm 6.28 years. The control group included five male and five female subjects. The control group had a mean age of 30.40 \pm 9.38 years. There were no significant differences in age or gender between the intractable TLE patients and controls (*p* > 0.05).

NL1 and NRX1 β Expression in Human Epileptogenic Tissue

Immunohistochemistry showed that the NL1 protein was expressed primarily in the membrane and cytoplasm of neurons in the temporal neocortex in control and intractable TLE groups. Faint and scattered NL1-immunoreactive staining was observed in the cytoplasm of cells from control subjects, whereas strong NL1 immunoreactivity was present in cells from individuals with intractable TLE (Fig. 1a). No

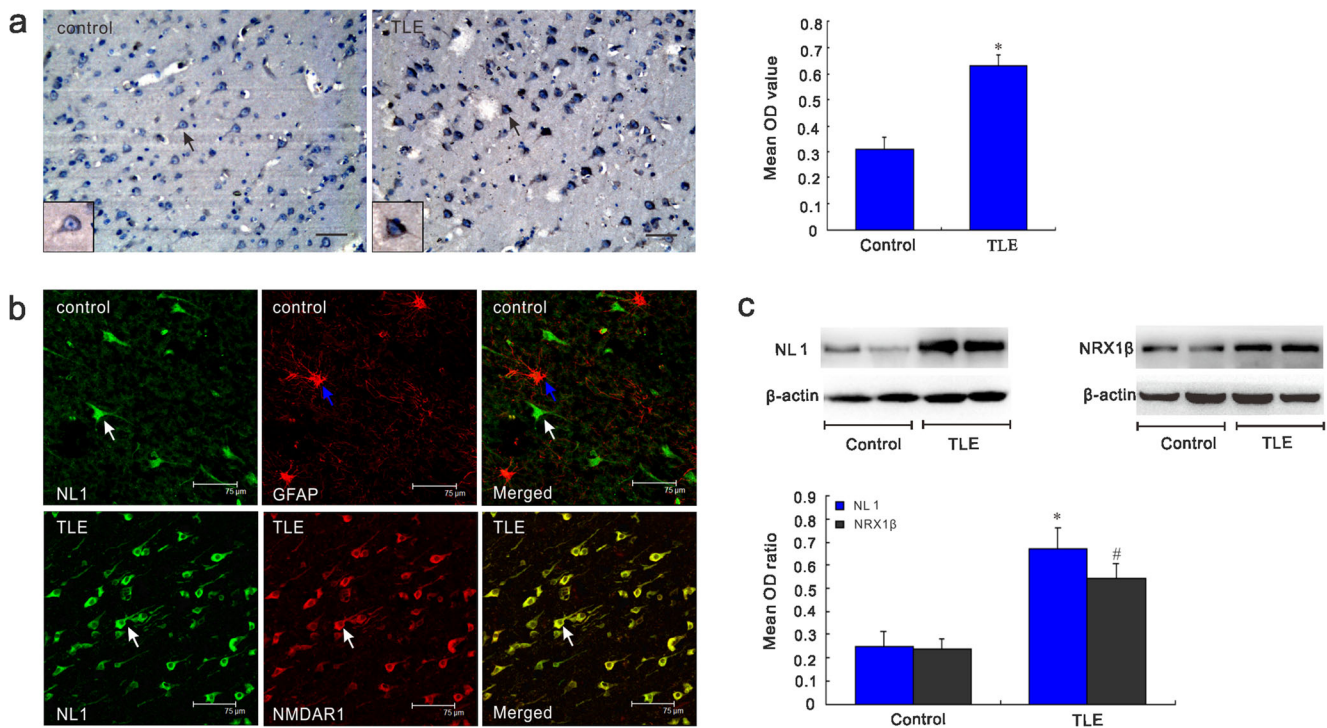


Fig. 1 NL1 and NRX1 β immunoreactivity in the temporal cortex of control subjects and subjects with intractable TLE. **a** NL1 immunohistochemical staining was faint and mainly expressed in neurons in control subjects, but staining was strong in intractable TLE patients. The white arrows indicate neurons. The blue arrows indicate astrocytes. The scale bar indicates 75 μ m. The mean OD value for NL1 was significantly higher in the temporal neocortex of the TLE group compared to the control group ($p<0.05$). **b** Double-label immunofluorescence showed that NL1 (green) and GFAP (red) were not co-expressed in astrocytes. NL1 (green) and NMDAR1 (red) were co-expressed in neurons. The white arrows indicate neurons, and the blue arrows indicate astrocytes. **c** Representative western blots showing NL1 and NRX1 β expression in intractable TLE patients and controls. The mean OD ratios for NL1 and NRX1 β were significantly higher in the TLE group compared to the control group ($p<0.05$). **d** * $p<0.05$ indicates statistically significant differences between the TLE group and the control group

and GFAP (red) were not co-expressed in astrocytes. NL1 (green) and NMDAR1 (red) were co-expressed in neurons. The white arrows indicate neurons, and the blue arrows indicate astrocytes. **c** Representative western blots showing NL1 and NRX1 β expression in intractable TLE patients and controls. The mean OD ratios for NL1 and NRX1 β were significantly higher in the TLE group compared to the control group ($p<0.05$). **d** * $p<0.05$ indicates statistically significant differences between the TLE group and the control group

immunoreactivity was detected in the negative controls in which the primary antibody was omitted. Student's t test revealed that the mean optical density (OD) of NL1 was significantly higher in the temporal neocortex of the TLE group ($n=22$) than in that of the control group ($n=10$, $p<0.05$; Fig. 1a).

Double-label immunofluorescent staining was used to further determine the localization of NL1-positive cells. Immunofluorescence demonstrated that NL1 (green) and GFAP (red) were seldom co-expressed in astrocytes in the temporal neocortex of the control group (Fig. 1b). The NMDAR1 protein, which is an essential component of NMDARs, is an important marker of glutamatergic excitatory synapses. We found that NL1-positive cells (green) were co-expressed with NMDAR1 (red) in the TLE group (Fig. 1b).

Western blot analyses of brain homogenates were performed to investigate the elevated NL1 immunostaining in epileptic brain sections and to detect NRX1 β expression. The expression of NL1 and NRX1 β was strong in subjects with intractable TLE, but their expression was relatively weak in control subjects (Fig. 1c). The levels of expression of NL1 and NRX1 β were normalized by calculating the ratio of the OD of the protein bands to that of the corresponding β -actin band

(Fig. 1c). Student's t test showed that the mean OD ratios for NL1 and NRX1 β were significantly higher in the temporal neocortex of the TLE group ($n=22$) compared to the control group ($n=10$; $p<0.05$).

NL1 and NRX1 β Expression in a Rat Seizure Model

Rats underwent an acute period (1, 2, and 3 days) after lithium-pilocarpine-induced seizures that was followed by a seizure-free period termed the latent period (7, and 14 days), and then a SRS period, termed the chronic period (30, and 60 days). We investigated whether seizure activity affected NL1 and NRX1 β expression at these time points.

NL1 immunohistochemical staining was extensive in the neocortex and in all regions of the hippocampus, and intense hippocampal staining was observed in the dentate gyrus and in the CA1 and CA3 regions. Only faint staining was observed in the neocortex and hippocampus of controls (Fig. 2a). In experimental groups, the strongest NL1 immunoreactivity was observed predominantly in the membrane and cytoplasm of neurons in the temporal neocortex and hippocampus at 30 days post seizure (Fig. 2a). No staining was observed when the primary antibody was omitted. The mean OD value for NL1

expression in the hippocampus changed dynamically during different phases ($n=4$ per group; Fig. 2a). One-way ANOVA revealed significant differences in the mean OD for NL1 expression between groups ($p<0.05$). Tukey's HSD post hoc multiple comparison test showed that the difference in NL1 expression levels between the control and each treated group was significant ($p<0.05$), except for the 7-day and 14-day groups ($p>0.05$). There was a significant difference in NL1 expression levels between all pairs of treated groups ($p<0.05$), except between the 1- and 3-day groups, 2- and 3-day groups, 7- and 14-day groups, and 30- and 60-day groups and among the 2-, 30- and 60-day groups ($p>0.05$).

Double-labeling immunofluorescence showed that NL1-positive cells (green) were not co-expressed with GFAP (red) in astrocytes in the control group, but NL1 was co-expressed with NMDAR1 (red) in neurons in the TLE group (Fig. 2b).

Western blot analyses of rat hippocampal extracts were performed ($n=4$ per group) to further confirm the alterations in NL1 expression that were observed by immunohistochemical staining and to detect NRX1 β expression. As shown in Fig. 2c, compared with the controls, both NL1 expression and NRX1 β expression were elevated during the acute period (1, 2, 3 days) and the chronic period (30, 60 days) in the TLE group, and the expression profiles of NL1 and NRX1 β were almost identical. NL1 and NRX1 β expression was normalized by calculating the ratio of the OD of the bands to the corresponding β -actin band (Fig. 2c). One-way ANOVA showed significant differences in the mean OD ratio for NL1 among the groups ($p<0.05$). Tukey's HSD post hoc multiple comparison test showed that the difference in NL1 expression level in the hippocampus between the control group and every treated group was significant ($p<0.05$), with the exception of the 7- and 14-day groups ($p>0.05$). There were significant differences in the mean OD ratios for NL1 between all pairs of treated group ($p<0.05$), except between the 1- and 3-day groups, 1- and 7-day groups, 2- and 3-day groups, 2- and 60-day groups, and 30- and 60-day groups ($p>0.05$). One-way ANOVA also showed that there were significant differences in NRX1 β expression between groups ($p<0.05$). Tukey's HSD post hoc multiple comparison test showed a significant difference in NRX1 β expression between the control group and every treated group ($p<0.05$) except the 7-day group ($p>0.05$). Differences in the mean OD ratios for NRX1 β between each and every treated group were significant ($p<0.05$), except between the 1- and 14-day groups, 2- and 3-day groups, and 30- and 60-day groups ($p>0.05$).

Analysis of NL1 and NRX1 β mRNA fold changes from different experimental groups was performed using the qRT-PCR method as shown in Fig. 2d ($n=4$ per group). One-way ANOVA showed significant differences in the mRNA fold change for NL1 among the groups ($p<0.05$). Tukey's HSD post hoc multiple comparison test showed that the difference

in NL1 mRNA fold change in the hippocampus between the control group and every treated group was significant ($p<0.05$), with the exception of the 7- and 14-day groups ($p>0.05$). There were significant differences in the mean OD ratios for NL1 between all pairs of treated group ($p<0.05$), except between the 1- and 3-day groups, 1- and 7-day groups, 2- and 3-day groups, 7- and 14-day groups, and 30- and 60-day groups ($p>0.05$). One-way ANOVA also showed that there were significant differences in NRX1 β mRNA fold change between groups ($p<0.05$). Tukey's HSD post hoc multiple comparison test showed a significant difference in NRX1 β mRNA fold change between the control group and every treated group ($p<0.05$) except the 7-day group ($p>0.05$). Differences in the mRNA fold change for NRX1 β between each and every treated group were significant ($p<0.05$), except between the 1- and 3-day groups, 1- and 7-day groups, 2- and 3-day groups, and 30- and 60-day groups ($p>0.05$).

NL1 Knockdown in the Hippocampus Decreased NL1 Expression in Normal Rats

Western blot analyses of rat hippocampal extracts were performed using an NL1-selective antibody at 1, 3, and 7 days after virus infusion to confirm that sh-NL1 successfully suppressed the expression of endogenous NL1 in the hippocampus *in vivo* (Fig. 3a). Rats treated with vehicle virus infusions at the corresponding time points were used as controls. NL1 expression was normalized by calculating the ratio of the OD of the NL1 bands to the corresponding β -actin bands ($n=4$ per group; Fig. 3a). Student's *t* test showed that the mean OD ratios for NL1 in the sh-NL1 group decreased significantly compared to the corresponding control group 3 and 7 days after infusion ($p<0.05$). There was no significant difference between the 3- and 7-day groups ($p>0.05$). Thus, the efficiency of RNA interference in knocking down NL1 expression *in vivo* became stable by day 7. The amount of NL1 decreased by 36.3 ± 4.3 and $44.2 \pm 5.3\%$ of control levels at 3 and 7 days after infusion, respectively. Immunofluorescent staining using an EGFP antibody was used to further determine whether the lentivirus had successfully transfected hippocampal neurons. Immunofluorescence showed that EGFP was localized in the hippocampus, especially in the CA1 area (Fig. 3c) and the dentate gyrus. Because the effects of RNA interference took several days to stabilize, we began lithium chloride-pilocarpine injections and performed rat behavioral investigations 7 days after virus infusion.

NL1 Knockdown in Epileptic Rats Reduced Seizure Severity and Prolonged Seizure Latency

Seizures were scored in 20-min intervals for 60 min after pilocarpine injection to evaluate seizure severity ($n=12$ per

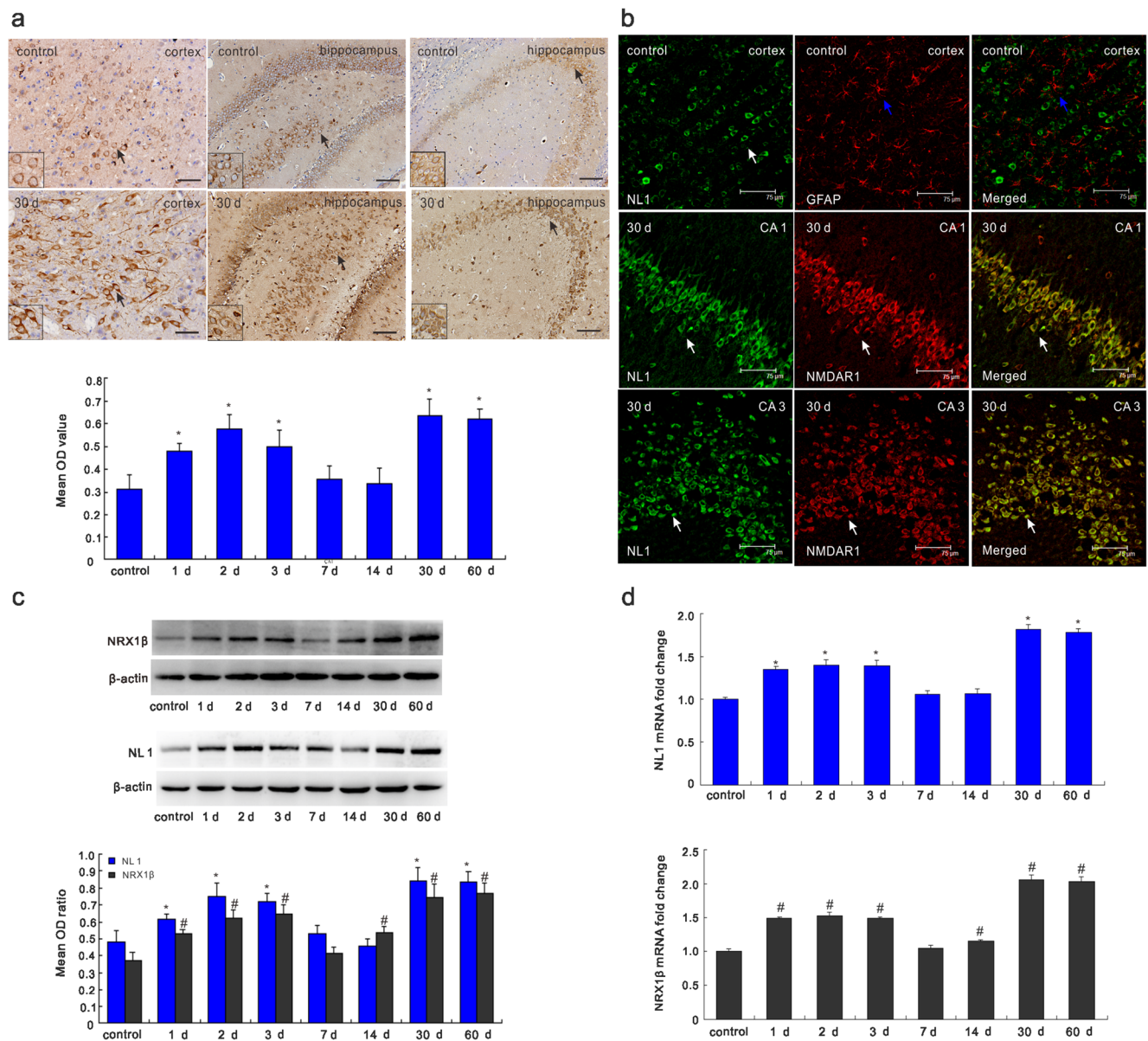


Fig. 2 NL1 and NRX1β immunoreactivity in the hippocampus and adjacent cortex of rats. **a** Faint immunohistochemical staining of NL1 was observed mainly in the cortex and the hippocampus of control rats, but strong NL1 immunoreactivity was predominantly observed in the membrane and cytoplasm of neurons in the cortex and hippocampus 30 days after seizures. The black arrows indicate neurons. The scale bar indicates 75 μm. The graph shows mean OD values at different time points after seizures in the rat hippocampus. **b** Double-label immunofluorescence in the rat cortex and hippocampus. NL1 (green) and GFAP (red) were not co-expressed in astrocytes. NL1 (green) and NMDAR1 (red)

(red) were co-expressed in neurons in the CA1 and CA3 regions. The white arrows indicate neurons, and the blue arrows indicate astrocytes. The scale bar indicates 75 μm. **c** Representative western blot showing the dynamics of NL1 and NRX1β expression at different time points after seizures in the hippocampus. The graph represents mean OD ratios for NL1 or NRX1β compared to β-actin. **d** The graphs show NL1 and NRX1β mRNA fold changes at different time points after seizures in the rat hippocampus. *#p<0.05 indicates significant differences between different time points for the treated and control groups

group; Fig. 3b). All rats developed more severe seizures over time. Repeated measures ANOVA revealed that seizures in the sh-NL1 group were less severe than those in the other groups in each 20-min interval ($p<0.05$). There was a significant main effect of time ($p<0.05$), but no significant time×group interaction was

observed ($p>0.05$), which suggests that seizures became progressively severe in these groups over time. However, the main effect of time did not affect the differences between these groups.

We observed the maximum Racine score during the 60-min trial ($n=12$ per group). One-way ANOVA showed that the

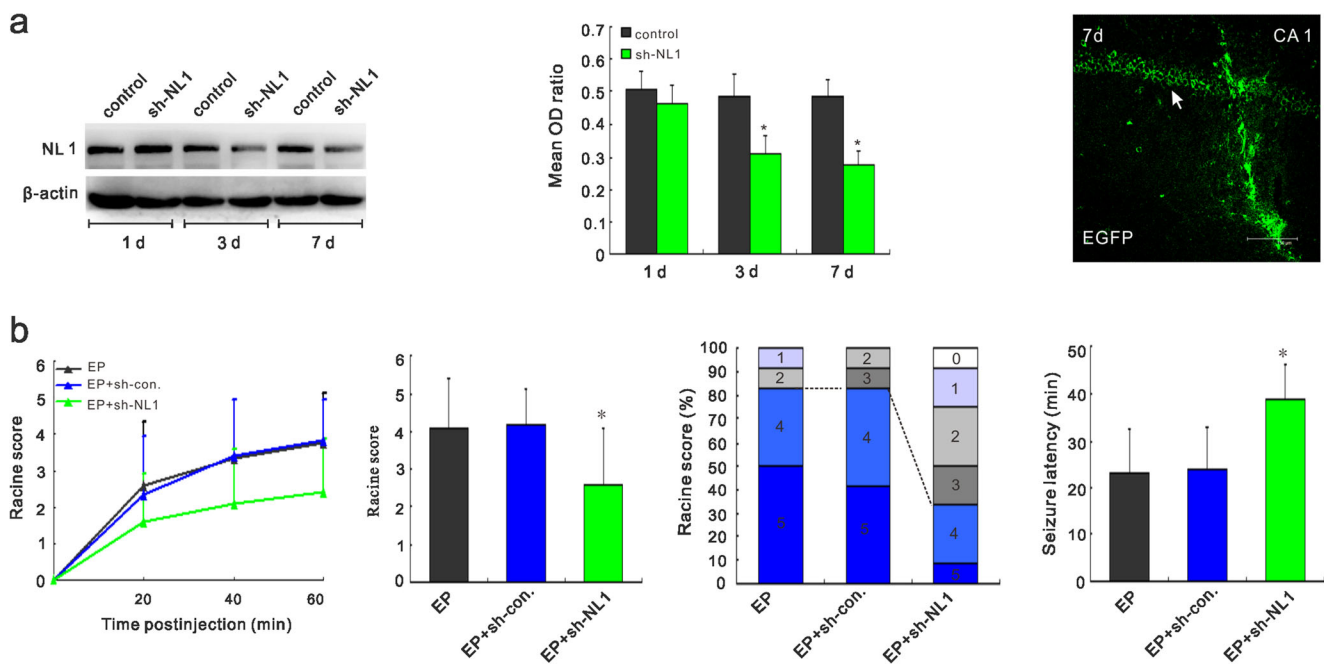


Fig. 3 Lentivirally mediated depletion of NL1 in the hippocampus decreased NL1 expression in normal rats and reduced seizures in epileptic rats post modeling after sh-NL1 infusion. **a** Western blot analyses showing the reduced expression of NL1 3 and 7 days after sh-NL1 infusion in normal rats. The rats with vehicle virus infusions at the corresponding time points were used as controls. Mean OD ratio values for NL1 in the sh-NL1 group were significantly decreased 3 and 7 days after infusion compared to the corresponding control groups ($p<0.05$). * $p<0.05$ indicates statistically significant differences between the OD values for the sh-NL1 group at each time point and the OD values for the corresponding control groups. Immunofluorescence showed that EGFP was localized in the CA1 area in the hippocampus 7 days after sh-NL1

infusions in normal rats. The scale bar indicates 150 μ m. **b** The highest Racine score of epileptic rats in the sh-NL1 epileptic group in each 20-min interval was less severe than that of the other groups. The maximum Racine score during the 60-min trial in the sh-NL1 group was lower than that of the other groups ($p<0.05$). The proportion of generalized clonic or tonic seizures (seizure score 4 or 5) in the sh-NL1 epileptic group was significantly lower than that in the other groups ($p<0.05$). NL1 knockdown significantly delayed seizure latency in the sh-NL1 epileptic group compared to the other groups ($p<0.05$). * $p<0.05$ indicates statistically significant differences between the sh-NL1 epileptic group and the epileptic group or sh-con epileptic group

maximum Racine score in the sh-NL1 epileptic group was less severe than that in the other groups ($p<0.05$), but there was no significant difference between the two control epileptic groups ($p>0.05$).

Finally, only 33.3 % of rats in the sh-NL1 epileptic group showed generalized clonic or tonic seizures (i.e., seizure scores of 4 or 5) compared to 83.3 % of the rats in both control groups. Fisher's exact test showed that NL1 knockdown significantly reduced the incidence of generalized clonic and tonic seizures ($p<0.05$).

Because NL1 was observed to affect seizure severity, we hypothesized that NL1 may also affect seizure latency. We tested this possibility by recording the time of onset of the first generalized clonic or tonic seizure ($n=12$ per group). One-way ANOVA followed by Tukey's HSD post hoc test revealed that NL1 knockdown significantly increased seizure latency compared to the control groups ($p<0.05$), but there was no significant difference between the two control groups ($p>0.05$). These results indicate that NL1-knockdown rats exhibited decreased seizure susceptibility.

NL1 Knockdown Decreased NL1 Expression in the Hippocampus and Inhibited Hyperexcitability in Hippocampal Slices 30 Days Post Modeling

NL1 expression reached a peak level during the chronic phase, which is the key stage for the development of drug-refractory epilepsy. Thus, we investigated the efficiency of NL1 knockdown by RNA interference *in vivo*. We prepared rat brain slices for electrophysiological assays from animals sacrificed 30 days after pilocarpine injection. Three epileptic groups given hippocampal injections of saline (EP), vehicle virus (EP+sh-con), or NL1 shRNA (EP+sh-NL1) and one normal control group given hippocampal injections of saline (control) were included in analyses of the efficiency of RNA interference. Western blot analyses of rat hippocampal extracts from the four groups 30 days after pilocarpine injection were performed using an anti-NL1 antibody (Fig. 4a). NL1 expression decreased significantly in the sh-NL1 epileptic group compared to the sh-con and epileptic groups ($p<0.05$). There were no significant differences between the sh-con epileptic group and the sh-NL1 epileptic group and the

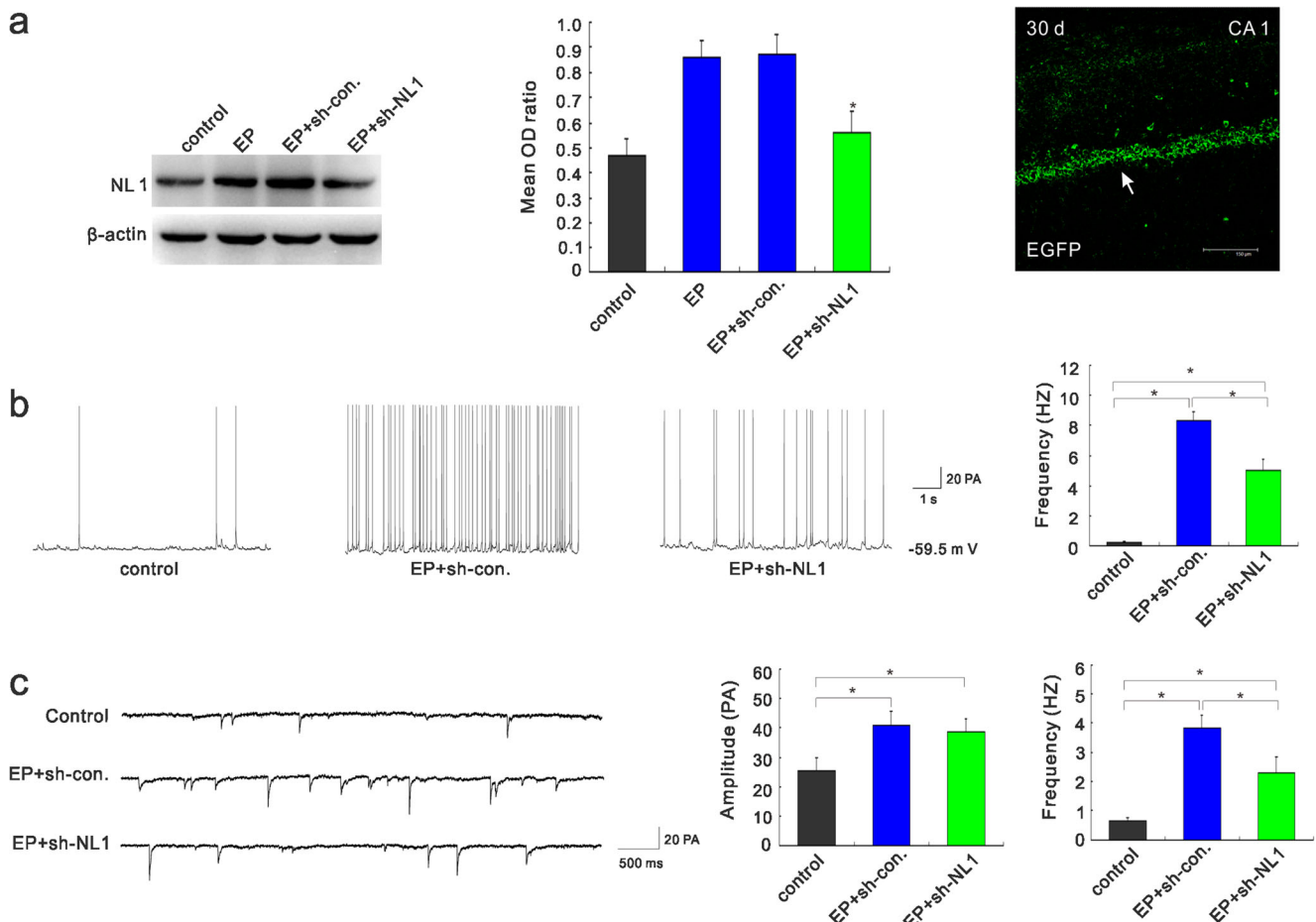


Fig. 4 NL1 knockdown in the hippocampi decreased NL1 expression and inhibited hyperexcitability in hippocampal slices in epileptic rats 30 days post modeling. **a** Western blot analyses of NL1 expression in the hippocampi in different groups. NL1 expression in the hippocampi was significantly decreased in the sh-NL1 epileptic group compared to the sh-con epileptic group and epileptic group ($p<0.05$). * $p<0.05$ indicates statistically significant differences between the sh-NL1 group and the epileptic group or sh-con epileptic group. Immunofluorescence

showed that EGFP was localized in the CA1 area of the hippocampus 30 days after pilocarpine injection. The scale bar indicates 150 μ m. **b** NL1 knockdown in epileptic rats at day 30 inhibits the frequency of spontaneous APs in CA1 pyramidal neurons in hippocampal slices. **c** NL1 knockdown in epileptic rats at day 30 reduces mEPSC frequency but not mEPSC amplitude in hippocampal slices. * $p<0.05$ indicates statistically significant differences between the two marked groups

normal control group ($p>0.05$, one-way ANOVA followed by Tukey's HSD post hoc test). In addition, EGFP immunofluorescence indicated that the lentivirus had successfully transfected hippocampal neurons (Fig. 4a).

Figure 4b shows that the frequency of spontaneous APs increased in the sh-con epileptic group ($n=10$, $p<0.05$) and the sh-NL1 epileptic group ($n=8$, $p<0.05$) compared to the normal control group ($n=8$). One-way ANOVA followed by Tukey's HSD post hoc test revealed that the frequency of spontaneous APs in the sh-NL1 epileptic group was lower than the sh-con epileptic group.

Figure 4c shows that the mean mEPSC amplitudes from the sh-con epileptic group ($n=10$) and the sh-NL1 epileptic group ($n=10$) increased significantly compared to the normal control group ($n=12$, $p<0.05$). There was no significant difference in the mean mEPSC amplitude between the sh-NL1

epileptic group and sh-con epileptic group ($p>0.05$). The mean mEPSC frequency in the sh-con epileptic group ($n=10$) and the sh-NL1 epileptic group ($n=10$) increased dramatically compared to the normal control group ($n=12$; $p<0.05$). The mEPSC frequency in the sh-NL1 epileptic group was lower than that in the sh-con epileptic group ($p<0.05$).

NL1 Knockdown in Epileptic Rats Selectively Reduced NMDAR-Mediated Synaptic Currents and Downregulated NMDAR1 Expression in the Hippocampus 30 Days Post Modeling

Representative traces show NMDAR-dependent EPSCs and AMPAR-dependent EPSCs from the control, sh-con epileptic, and sh-NL1 groups (Fig. 5a). We calculated synaptic NMDAR/AMPAR ratios to assess whether NL1 knockdown

in epileptic rats affected synaptic transmission in the hippocampus (Fig. 5b). The ratio in the sh-NL1 epileptic group ($n=8$) was significantly lower than those in the normal control group ($n=9$) and sh-con epileptic group ($n=9$). The decreased ratio in the sh-NL1 epileptic group may have resulted from either a selective decrease in NMDA synaptic currents or a selective increase in AMPA synaptic currents or both. We recorded amplitudes of NMDAR-dependent EPSCs and AMPAR-dependent EPSCs to distinguish between these possibilities (Fig. 5b). The sh-NL1 epileptic group showed a significant decrease in the average amplitude of NMDAR-dependent EPSCs, but not in the average amplitude of AMPAR-dependent EPSCs, compared to the sh-con epileptic group.

We examined total and surface receptor NMDAR1 expression in the hippocampus 30 days after pilocarpine injection using western blot analysis to investigate whether NL1 knockdown altered NMDAR expression levels (Fig. 5c). The total/ β -actin and surface/total ratios for NMDAR1 expression in the epileptic and sh-con epileptic groups were significantly higher than the corresponding ratios for the control group ($p<0.05$). However, the total/ β -actin and surface/total ratios for NMDAR1 protein expression in the sh-NL1 epileptic group were significantly lower than those in the epileptic and sh-con epileptic groups ($p<0.05$).

Discussion

Synapse formation is essential for the normal establishment and remodeling of neuronal circuitry in the brain, and impairments of synapse formation are important factors in the pathogenesis of brain disorders such as epilepsy [25]. A previous study found that the binding of NL1 to NRX1 β induces neurite outgrowth, which eventually induces the formation of excitatory neuronal circuits [26]. Recent research reports that NL1 knockdown reduces the survival of new hippocampal neurons arising from neurogenesis in adults and that this reduction in survival is associated with changes in dendrite and spine morphology during granule cell maturation [27]. Abnormal dendrite and spine morphology and the sprouting of mossy fibers, which establish critical interconnections and increase hyperexcitability, are associated with epilepsy [28, 29]. Thus, we sought to determine whether NL1 may be involved in the occurrence of TLE and, if so, to identify the mechanisms underlying this process.

Histopathological findings in our research revealed NL1 immunopositivity in neurons and co-expression with NMDAR1 in the temporal lobe tissues of humans and rats; these studies were complementary to a previous study in rats brains [30]. We showed that the upregulation of NL1 in the hippocampus after seizures was predominantly limited to the

dentate gyrus and the CA1 and CA3 regions. These data indicate that NL1 likely plays a role in TLE through the activation of specific neurons in the hippocampus, which is quite susceptible to seizures. The experimental evidence for the involvement of NL1 in seizures in our study is based on the anticonvulsant activity of lentivirally mediated NL1 knockdown during the acute phase of epileptogenesis. Epileptogenesis refers to a dynamic process that progressively alters excitability in neuronal circuitry [2], and this early control of the first seizure using NL1 suppression in the acute phase may alleviate epileptogenesis, including the chronic phase that is characterized by SRS. Moreover, our data showed similarly increased expression of NL1 and NRXN1 β in TLE patients and rats in the chronic phase. We also investigated the contribution of NL1 knockdown in epileptic rats to antiepileptogenesis in the chronic phase.

Synaptic reorganization of the CA1 axons that project to the subiculum, which is the final output channel of the hippocampus, could potentially play a major role in the persistent cellular hyperexcitability observed in epileptic hippocampal circuitry [31]. Thus, our electrophysiological study in hippocampal slices focused on CA1 pyramidal neurons, which are most affected in TLE in the chronic phase. Our electrophysiological experimental procedures did not cut the axons that projected from CA3/CA2. Thus, the APs and mEPSCs that were observed resulted from spontaneous transmitter release from local axons and projection axons. We observed an increased frequency of spontaneous APs in epileptic rats. However, NL1 suppression *in vivo* significantly reduced the AP frequency in epileptic rats. The frequency of mEPSCs is likely determined by presynaptic factors, while the amplitude of mEPSCs is controlled by postsynaptic mechanisms. We found an increase in the frequency and amplitude of mEPSCs in epileptic rats, which suggests that increased numbers of presynaptic axon terminals synapsed on CA1 pyramidal neurons and that increased numbers of postsynaptic receptors were available in CA1 neurons. However, NL1 knockdown in epileptic rats resulted in a decrease in mEPSC frequency but not amplitude, which suggests that NL1 knockdown decreased the number of axon terminals from the projection axons of the CA3 region or of newly formed local excitatory circuits; these decreases may have resulted from the sprouting of recurrent CA1 axon collaterals during epileptogenesis [32]. Therefore, lentivirally mediated NL1 knockdown may reduce the hyperexcitability of epileptic CA1 neurons; such a reduction would also decrease excitation in the hippocampus and reduce the occurrence of SRS.

A previous study revealed that the activation of postsynaptic NMDARs and CaM-Kinase II signaling downstream is essential for NL1 to enhance synaptic function in neurons [10]. NMDARs and CaM-Kinase II activation have previously been implicated in the modulation of seizure activity as well [33, 34]. We hypothesized that lentivirally mediated NL1

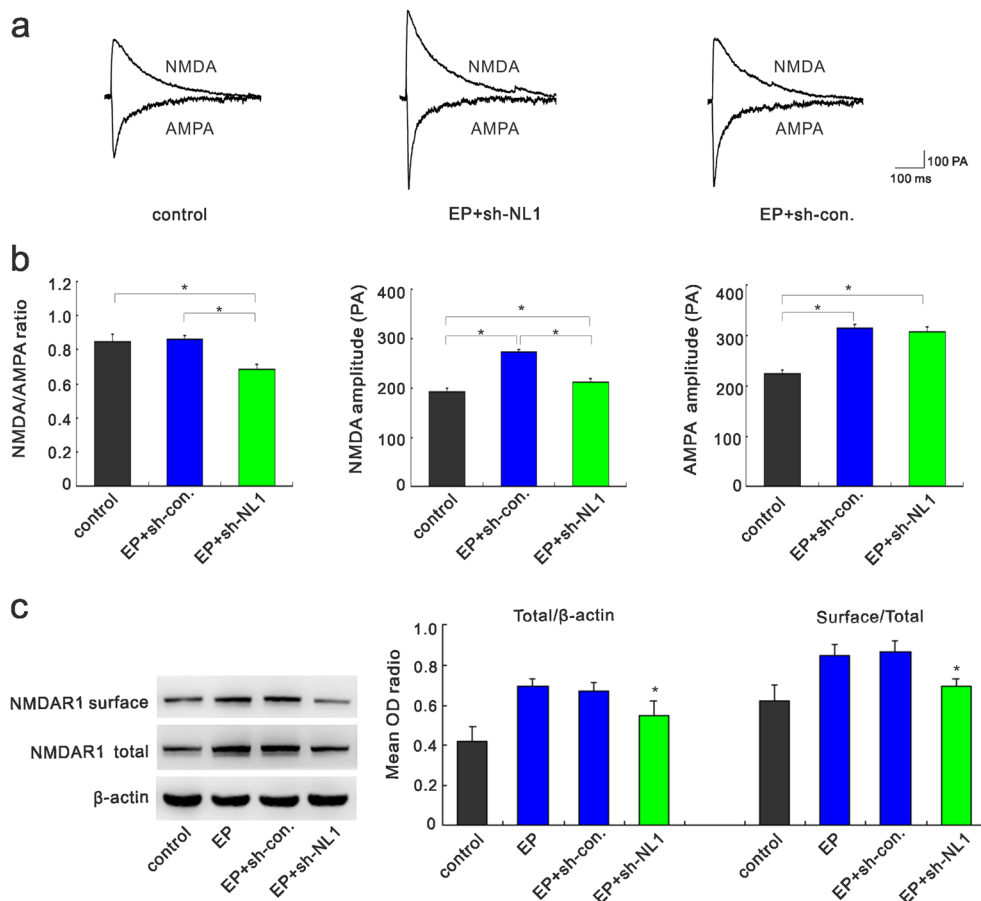


Fig. 5 NL1 knockdown in epileptic rats selectively reduces NMDAR-mediated synaptic currents and downregulates NMDAR1 expression in the hippocampi 30 days post modeling. **a** Representative traces of NMDAR-dependent EPSCs and AMPAR-dependent EPSCs from the control, sh-con epileptic, and sh-NL1 groups. **b** The NMDAR/AMPAR ratio in the sh-NL1 epileptic group was significantly lower than that in the control groups. The sh-NL1 epileptic group exhibited a significant decrease in the average amplitude of NMDAR-dependent EPSCs, but not AMPAR-dependent EPSCs, compared to the sh-con epileptic group.

* $p<0.05$ indicates statistically significant differences between the two groups marked. **c** The total/β-actin and surface/total ratios for NMDAR1 expression in the epileptic and sh-con epileptic groups were significantly greater than those in the control group ($p<0.05$). The total/β-actin and surface/total ratios for NMDAR1 protein expression in the sh-NL1 epileptic group were significantly lower than those in the epileptic and sh-con epileptic groups ($p<0.05$). * $p<0.05$ indicates statistically significant differences between the sh-NL1 group and the epileptic group or the sh-con epileptic group

depletion in epileptic hippocampi would suppress NMDAR function. Accordingly, we found that NL1 knockdown in epileptic rats decreased NMDAR/AMPAR ratios and specifically reduced NMDAR-mediated synaptic transmission. This result is consistent with a previous report that the NMDAR/AMPAR ratio is selectively decreased in the CA1 area in NL1 knockout mice [10]. This phenomenon suggests that the observed alteration in excitatory currents was caused by changes in the numbers of excitatory glutamate receptor.

New research provides evidence that synaptic NMDAR number and subunit composition are not static but instead change dynamically in response to neuronal activity, which can contribute to neuropsychiatric disorders if this activity is dysregulated [35]. NMDARs consist of at least one obligatory NMDAR1 and one or more NMDAR GluN2 subunits [36]. NMDAR1 is the most widely distributed NMDAR subunit in

the adult rat hippocampus [37]. Notably, our study showed that the suppression of NL1 reduced the total and surface/total ratios for NMDAR1 expression in epileptic hippocampi; this finding is of interest because no significant change in NMDAR subunits has been observed in NL1 knockout mice [38]. Recently, the results of a co-immunoprecipitation study in heterologous cells and of proximity ligation assays suggest that NL1, but not NL2 or NL3, plays a unique, instructive role in the control of the synaptic abundance of NMDARs at glutamatergic synapses via binding to NMDAR1 [39]. Therefore, NL1 may regulate NMDAR expression through direct interactions with NMDAR1. We speculate that the decreased frequencies of NMDAR-dependent EPSCs observed in NL1 knockdown epileptic hippocampi are partly attributable to decreased total NMDAR1 number and altered NMDAR1 trafficking from the plasma membrane to the cytoplasm. The decreased numbers of NMDARs may affect glutamatergic

excitatory synaptic transmission and induce a decrease in the overall hyperexcitability of the epileptic hippocampus.

The human tissue data used in our study have some limitations. We used structurally normal brain tissue from temporal lobectomies that were performed for the treatment of traumatic brain injuries as our control samples due to practical and ethical considerations associated with obtaining normal human brain specimens. Brain specimens from TLE patients could only be obtained during the drug-resistant stage of epilepsy. The rat model of lithium-pilocarpine-induced seizures is widely used as a model for human TLE, and this model could be used to shed more light on the pathological changes and molecular cascades that lead to TLE. Thus, we used two complementary approaches in this study; we examined brain tissues from both TLE patients and experimental animals.

Taken together, the results of our study of intractable TLE patients revealed that the levels of expression of the NL1 and NRX1 β proteins were increased in temporal lobe epileptic foci. NL1 and NRX1 β protein and mRNA levels were elevated during the acute period in epileptic rats, and a lentivirally mediated intervention prevented NL1 upregulation and reduced seizures after pilocarpine injection. These results demonstrate that dysregulation of NL1 is a trigger for the induction of seizures rather than a consequence of seizures and that the downregulation of NL1 prevented seizures. NL1 and NRX1 β protein and mRNA levels peaked during the chronic phase. NL1 knockdown in epileptic rats during the chronic phase inhibited the hyperexcitability of CA1 pyramidal neurons in hippocampal slices; this finding indicates that the suppression of NL1 decreased synchrony and ameliorated the faster propagation of epileptic discharges within the hippocampus. However, further study is required to understand the precise mechanisms by which NL1 modulates synaptic transmission in epileptic rats.

Acknowledgments This work was supported by National Natural Science Foundation Of China (grant numbers are 81401070, 81471319, and 81301630). The authors sincerely thank the patients and their families for their participation in this study. We thank the Xinqiao Hospital of the Third Military Medical University, Beijing Tiantan Hospital and Xuanwu Hospital of the Capital University of Medical Sciences for their support in brain tissue procurement, and the National Institutes of Health of China and the Ethics Committee on Human Research of the Chongqing Medical University.

Conflict of Interest The authors declare that they have no conflict of interest.

References

- Sander JW (2003) The epidemiology of epilepsy revisited. *Curr Opin Neurol* 16(2):165–170. doi:[10.1097/01.wco.0000063766.15877.8e](https://doi.org/10.1097/01.wco.0000063766.15877.8e)
- Fisher RS, van Boas EW, Blume W, Elger C, Genton P, Lee P, Engel Jr (2005) Epileptic seizures and epilepsy: definitions proposed by the International League Against Epilepsy (ILAE) and the International Bureau for Epilepsy (IBE). *Epilepsia* 46(4):470–472. doi:[10.1111/j.0013-9580.2005.66104.x](https://doi.org/10.1111/j.0013-9580.2005.66104.x)
- Esclapez M, Hirsch JC, Ben-Ari Y, Bernard C (1999) Newly formed excitatory pathways provide a substrate for hyperexcitability in experimental temporal lobe epilepsy. *J Comp Neurol* 408(4):449–460. doi:[10.1002/\(SICI\)1096-9861\(19990614\)408:4<449::AID-CNE1>3.0.CO;2-R](https://doi.org/10.1002/(SICI)1096-9861(19990614)408:4<449::AID-CNE1>3.0.CO;2-R)
- Dalva MB, McClelland AC, Kayser MS (2007) Cell adhesion molecules: signalling functions at the synapse. *Nat Rev Neurosci* 8(3):206–220. doi:[10.1038/nrn2075](https://doi.org/10.1038/nrn2075)
- Krueger DD, Tuffy LP, Papadopoulos T, Brose N (2012) The role of neurexins and neuroligins in the formation, maturation, and function of vertebrate synapses. *Curr Opin Neurobiol* 22(3):412–422. doi:[10.1016/j.conb.2012.02.012](https://doi.org/10.1016/j.conb.2012.02.012)
- Bottos A, Rissone A, Bussolino F, Arese M (2011) Neurexins and neuroligins: synapses look out of the nervous system. *Cell Mol Life Sci*. doi:[10.1007/s0018-011-0664-z](https://doi.org/10.1007/s0018-011-0664-z)
- Ichchenko K, Hata Y, Nguyen T, Ullrich B, Missler M, Moomaw C, Sudhof TC (1995) Neuroligin 1: a splice site-specific ligand for beta-neurexins. *Cell* 81(3):435–443
- Bolliger MF, Frei K, Winterhalter KH, Gloor SM (2001) Identification of a novel neuroligin in humans which binds to PSD-95 and has a widespread expression. *Biochem J* 356(Pt 2):581–588
- Arac D, Boucard AA, Ozkan E, Strop P, Newell E, Sudhof TC, Brunger AT (2007) Structures of neuroligin-1 and the neuroligin-1/neurexin-1 beta complex reveal specific protein-protein and protein-Ca²⁺ interactions. *Neuron* 56(6):992–1003. doi:[10.1016/j.neuron.2007.12.002](https://doi.org/10.1016/j.neuron.2007.12.002)
- Chubykin AA, Atasoy D, Etherton MR, Brose N, Kavalali ET, Gibson JR, Sudhof TC (2007) Activity-dependent validation of excitatory versus inhibitory synapses by neuroligin-1 versus neuroligin-2. *Neuron* 54(6):919–931. doi:[10.1016/j.neuron.2007.05.029](https://doi.org/10.1016/j.neuron.2007.05.029)
- Levinson JN, Chery N, Huang K, Wong TP, Gerrow K, Kang R, Prange O, Wang YT, El-Husseini A (2005) Neuroligins mediate excitatory and inhibitory synapse formation: involvement of PSD-95 and neurexin-1beta in neuroligin-induced synaptic specificity. *J Biol Chem* 280(17):17312–17319. doi:[10.1074/jbc.M413812200](https://doi.org/10.1074/jbc.M413812200)
- Chih B, Engelman H, Scheiffele P (2005) Control of excitatory and inhibitory synapse formation by neuroligins. *Science* 307(5713):1324–1328. doi:[10.1126/science.1107470](https://doi.org/10.1126/science.1107470)
- Wittenmayer N, Korber C, Liu H, Kremer T, Varoqueaux F, Chapman ER, Brose N, Kuner T, Dresbach T (2009) Postsynaptic Neuroligin1 regulates presynaptic maturation. *Proc Natl Acad Sci U S A* 106(32):13564–13569. doi:[10.1073/pnas.0905819106](https://doi.org/10.1073/pnas.0905819106)
- Stan A, Pielarski KN, Brigadski T, Wittenmayer N, Fedorchenco O, Gohla A, Lessmann V, Dresbach T, Gottmann K (2010) Essential cooperation of N-cadherin and neuroligin-1 in the transsynaptic control of vesicle accumulation. *Proc Natl Acad Sci U S A* 107(24):11116–11121. doi:[10.1073/pnas.0914233107](https://doi.org/10.1073/pnas.0914233107)
- Pan Y, Liu G, Fang M, Shen L, Wang L, Han Y, Shen D, Wang X (2010) Abnormal expression of netrin-G2 in temporal lobe epilepsy neurons in humans and a rat model. *Exp Neurol* 224(2):340–346. doi:[10.1016/j.expneuro.2010.04.001](https://doi.org/10.1016/j.expneuro.2010.04.001)
- Fukata Y, Adesnik H, Iwanaga T, Bredt DS, Nicoll RA, Fukata M (2006) Epilepsy-related ligand/receptor complex LGI1 and ADAM22 regulate synaptic transmission. *Science* 313(5794):1792–1795. doi:[10.1126/science.1129947](https://doi.org/10.1126/science.1129947)
- Bie B, Wu J, Yang H, Xu JJ, Brown DL, Naguib M (2014) Epigenetic suppression of neuroligin 1 underlies amyloid-induced memory deficiency. *Nat Neurosci* 17(2):223–231. doi:[10.1038/nn.3618](https://doi.org/10.1038/nn.3618)

18. Sudhof TC (2008) Neuroligins and neurexins link synaptic function to cognitive disease. *Nature* 455(7215):903–911. doi:[10.1038/nature07456](https://doi.org/10.1038/nature07456)
19. Harrison V, Connell L, Hayesmoore J, McParland J, Pike MG, Blair E (2011) Compound heterozygous deletion of NRXN1 causing severe developmental delay with early onset epilepsy in two sisters. *Am J Med Genet A* 155A(11):2826–2831. doi:[10.1002/ajmg.a.34255](https://doi.org/10.1002/ajmg.a.34255)
20. Etherton MR, Tabuchi K, Sharma M, Ko J, Sudhof TC (2011) An autism-associated point mutation in the neuroligin cytoplasmic tail selectively impairs AMPA receptor-mediated synaptic transmission in hippocampus. *EMBO J.* doi:[10.1038/embj.2011.182](https://doi.org/10.1038/embj.2011.182)
21. Ching MS, Shen Y, Tan WH, Jeste SS, Morrow EM, Chen X, Mukaddes NM, Yoo SY, Hanson E, Hundley R, Austin C, Becker RE, Berry GT, Driscoll K, Engle EC, Friedman S, Gusella JF, Hisama FM, Irons MB, Lafiosca T, LeClair E, Miller DT, Neessen M, Picker JD, Rappaport L, Rooney CM, Sarco DP, Stoler JM, Walsh CA, Wolff RR, Zhang T, Nasir RH, Wu BL (2010) Deletions of NRXN1 (neurexin-1) predispose to a wide spectrum of developmental disorders. *Am J Med Genet B Neuropsychiatr Genet* 153B(4):937–947. doi:[10.1002/ajmg.b.31063](https://doi.org/10.1002/ajmg.b.31063)
22. Brooks-Kayal A (2010) Epilepsy and autism spectrum disorders: are there common developmental mechanisms? *Brain Dev* 32(9):731–738. doi:[10.1016/j.braindev.2010.04.010](https://doi.org/10.1016/j.braindev.2010.04.010)
23. Kim J, Jung SY, Lee YK, Park S, Choi JS, Lee CJ, Kim HS, Choi YB, Scheiffele P, Bailey CH, Kandel ER, Kim JH (2008) Neuroligin-1 is required for normal expression of LTP and associative fear memory in the amygdala of adult animals. *Proc Natl Acad Sci U S A* 105(26):9087–9092. doi:[10.1073/pnas.0803448105](https://doi.org/10.1073/pnas.0803448105)
24. Woldbye DP, Angehagen M, Gotzsche CR, Elbrond-Bek H, Sorensen AT, Christiansen SH, Olesen MV, Nikitidou L, Hansen TV, Kanter-Schlifke I, Kokka M (2010) Adeno-associated viral vector-induced overexpression of neuropeptide Y Y2 receptors in the hippocampus suppresses seizures. *Brain* 133(9):2778–2788. doi:[10.1093/brain/awq219](https://doi.org/10.1093/brain/awq219)
25. Fang M, Xi ZQ, Wu Y, Wang XF (2011) A new hypothesis of drug refractory epilepsy: neural network hypothesis. *Med Hypotheses* 76(6):871–876. doi:[10.1016/j.mehy.2011.02.039](https://doi.org/10.1016/j.mehy.2011.02.039)
26. Gjorlund MD, Nielsen J, Pankratova S, Li S, Korshunova I, Bock E, Berezin V (2012) Neuroligin-1 induces neurite outgrowth through interaction with neurexin-1beta and activation of fibroblast growth factor receptor-1. *FASEB J* 26(10):4174–4186. doi:[10.1096/fj.11-202242](https://doi.org/10.1096/fj.11-202242)
27. Schnell E, Long TH, Bensen AL, Washburn EK, Westbrook GL (2014) Neuroligin-1 knockdown reduces survival of adult-generated newborn hippocampal neurons. *Front Neurosci* 8:71. doi:[10.3389/fnins.2014.00071](https://doi.org/10.3389/fnins.2014.00071)
28. Smith BN, Dudek FE (2002) Network interactions mediated by new excitatory connections between CA1 pyramidal cells in rats with kainate-induced epilepsy. *J Neurophysiol* 87(3):1655–1658
29. Penzes P, Cahill ME, Jones KA, VanLeeuwen JE, Woolfrey KM (2011) Dendritic spine pathology in neuropsychiatric disorders. *Nat Neurosci* 14(3):285–293. doi:[10.1038/nn.2741](https://doi.org/10.1038/nn.2741)
30. Song JY, Ichtchenko K, Sudhof TC, Brose N (1999) Neuroligin 1 is a postsynaptic cell-adhesion molecule of excitatory synapses. *Proc Natl Acad Sci U S A* 96(3):1100–1105
31. Lehmann TN, Gabriel S, Kovacs R, Eilers A, Kivi A, Schulze K, Lanksch WR, Meencke HJ, Heinemann U (2000) Alterations of neuronal connectivity in area CA1 of hippocampal slices from temporal lobe epilepsy patients and from pilocarpine-treated epileptic rats. *Epilepsia* 41(Suppl 6):S190–S194
32. Perez Y, Morin F, Beaulieu C, Lacaille JC (1996) Axonal sprouting of CA1 pyramidal cells in hyperexcitable hippocampal slices of kainate-treated rats. *Eur J Neurosci* 8(4):736–748
33. Kalia LV, Kalia SK, Salter MW (2008) NMDA receptors in clinical neurology: excitatory times ahead. *Lancet Neurol* 7(8):742–755. doi:[10.1016/S1474-4422\(08\)70165-0](https://doi.org/10.1016/S1474-4422(08)70165-0)
34. Churn SB, Sombati S, Jakoi ER, Severt L, DeLorenzo RJ (2000) Inhibition of calcium/calmodulin kinase II alpha subunit expression results in epileptiform activity in cultured hippocampal neurons. *Proc Natl Acad Sci U S A* 97(10):5604–5609. doi:[10.1073/pnas.080071697](https://doi.org/10.1073/pnas.080071697)
35. Lau CG, Zukin RS (2007) NMDA receptor trafficking in synaptic plasticity and neuropsychiatric disorders. *Nat Rev Neurosci* 8(6):413–426. doi:[10.1038/nrn2153](https://doi.org/10.1038/nrn2153)
36. Seuberg PH (1993) The TINS/TiPS Lecture. The molecular biology of mammalian glutamate receptor channels. *Trends Neurosci* 16(9):359–365
37. Tovar KR, Westbrook GL (1999) The incorporation of NMDA receptors with a distinct subunit composition at nascent hippocampal synapses in vitro. *J Neurosci* 19(10):4180–4188
38. Blundell J, Blaiss CA, Etherton MR, Espinosa F, Tabuchi K, Walz C, Bolliger MF, Sudhof TC, Powell CM (2010) Neuroligin-1 deletion results in impaired spatial memory and increased repetitive behavior. *J Neurosci* 30(6):2115–2129. doi:[10.1523/JNEUROSCI.4517-09.2010](https://doi.org/10.1523/JNEUROSCI.4517-09.2010)
39. Budreck EC, Kwon OB, Jung JH, Baudouin S, Thommen A, Kim HS, Fukazawa Y, Harada H, Tabuchi K, Shigemoto R, Scheiffele P, Kim JH (2013) Neuroligin-1 controls synaptic abundance of NMDA-type glutamate receptors through extracellular coupling. *Proc Natl Acad Sci U S A* 110(2):725–730. doi:[10.1073/pnas.1214718110](https://doi.org/10.1073/pnas.1214718110)